Pergamon

Spectrochimica Acta, Vol. 50A, No. 6, pp. 1015–1022, 1994
Elsevier Science Ltd. Printed in Great Britain
0584–8539/94 $7.00 + 0.00

Selective site deuteration on the sugar ring as an efficient marker of conformation in nucleosides: the C–D stretching mode of the (2′-R)-[2′-^{2}H]-2′-deoxyuridine and its 3′,5′-O-(1,1,3,3-tetraisopropyldisiloxan-1,3-diyl)-derivative

L. GRAJCAR* and M. H. BARON

Laboratoire de Spectrochimie Infrarouge et Raman, CNRS, 2 rue Henri Dunant, 94320 Thiais, France

S. BECOUARN, S. CZERNECKI and J. M. VALERY

Laboratorie de Chimie des Glucides, Université Pierre et Marie Curie, T 74-E 6, 4 place Jussieu, 75005 Paris, France

and

C. REISS

Institut Jacques Monod, T 43, Université Paris VII, 2 place Jussieu, 75005 Paris, France

(*Received* 9 *August* 1993; *accepted* 17 *September* 1993)

Abstract—A uridine specifically deuterated on the deoxyribose ring at the C2′, and the same compound in a more rigid form, due to a chemically fused ring (between C3′ and C5′), have been synthesized. By NMR, the coupling constants $J_{1'-2'}$ and $J_{3'-4'}$ have been determined and the populations of the C2′-endo and C3′-endo conformers have been deduced for the two compounds. Comparison of these results with an FTIR and Raman study of the stretching mode νC–D on the C2′ site allows a specific assignment of each observed band to one of the two classes of conformers. This enables us to consider the further step: the direct recognition, by IR and Raman spectroscopies, of the *local* conformation at a specific site of a synthetic oligonucleotide, using the νCD signals as marker bands.

INTRODUCTION

PRECISE local conformation of the DNA double helix, as well as its *trans*-conformations, seems to play an essential role in most of the processes involved in genetic reactions. In particular, in DNA–protein interactions, specific mutual recognition of the reactants in well-defined spatial structures is required. Then, the knowledge of the conformational behaviour of the reactants at a molecular level is necessary to understand their activity.

For this purpose considerable efforts have been made, using some biochemical but mostly physical methods. X-ray diffraction [1], NMR [2–4] and photonic spectroscopy [5] are the most commonly used and have been the most fruitful. DNA vibrational spectroscopy combines interesting features: high sensitivity to conformations, minimal sample quantities, solid state and solution studies and kinetic measurements. Results already obtained by this technique show that some parts of the vibrational spectra (600–1800 cm^{-1}) account for global conformation of the double helix [5]. However, neither this method nor the other physical techniques enable one to observe a physical item characteristic of the local DNA conformation at the level of any specific nucleoside. X-ray diffraction experiments on single crystal or fibre samples as well as 2D NMR studies require heavy computational treatments of the data to provide the conformational parameters at the level of a specific nucleoside [4, 6–8].

The right-handed DNA helical structures can be broadly classified into two generically different categories, the A- and B-type families. The essential distinction between A- and B-type polynucleotide helices lies in the sugar puckering structure, C3′-endo for A families and C2′-endo (or a minor variant) for B families [5, 9, 10(a)]. In the left-handed DNA helices, of the Z-type, the sugar conformation may be C2′-endo or C3′-endo

* Author to whom correspondence should be addressed.

(2'-R)-[2'-^{2}H]-2'-deoxy-3',5'-*O*-(1,1,3,3-tetraisopropyldisiloxan-1,3-diyl)-β-D-uridine

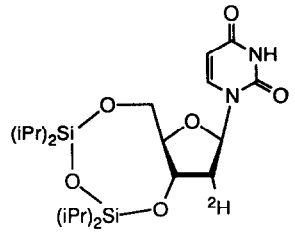

1

(2'-R)-[2'-^{2}H]-2'-deoxy-β-D-uridine

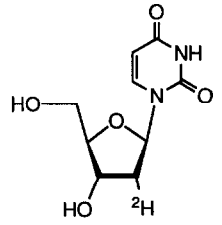

2

Fig. 1. Chemical structures of (2'-R)-[2'-^{2}H]-2'-deoxy-3',5'-O-TPDS-β-D-uridine, **1**, and (2'-R)-[2'-^{2}H]-2'-deoxy-β-D-uridine, **2**.

according to the sub-class [10(b)]. The geometry of the furanose ring is entirely described in the frame of the concept of pseudorotation by two parameters, the phase angle P and the amplitude τ_m of pseudorotation [11, 12]. Both experimental and theoretical studies display two main ranges of pseudorotational angle P, giving two preferred types of sugar puckering conformations, the C2'-endo (or S-type) and the C3'-endo (or N-type), corresponding to two minima in the calculated potential surfaces [13].

From the compilation of numerous X-ray studies of DNA fibres and of oligomer crystal structures [10, Tables 9.2 and 9.3 therein], all the DNA helical parameters appear to be interrelated by means of empirical correlations with the sugar puckering and the type of base sequence [10(c)], showing that conformational changes in helical polynucleotides are associated with concerted motions of all the torsion angles [10(d)].

All the experimental and modelling studies lead to the conclusion that the sugar puckering is correlated to a large extent to the conformation of the backbone and that consequently a local footprint informative on the sugar puckering of a specific nucleoside should enable one to infer the double helix structure in its close environment. Furthermore, it is remarkable that the conformational angles observed for polynucleotides occur in the same narrow ranges as in mononucleotides and mononucleosides [14].

As our goal is to use vibrational spectroscopy to tentatively characterize the local conformation of a double helix at the site of a chosen base of an oligonucleotide, isolated or complexed, a preliminary step consists of studying the conformational behaviour of nucleosides.

As the νCD stretching frequency is known to be sensitive to the conformations of the molecular environment of the C–D bond [15, 16] we thought to deuterate selectively one particular carbon of the deoxyribose ring in a nucleoside. Moreover, the νCD mode occurring in a spectral region (between 2100 and 2350 cm^{-1}) different from those of all the fundamental vibrations of DNA, proteins, lipids and water ($<1800\,cm^{-1}$ and $>2500\,cm^{-1}$), its observation was expected to be unambiguous.

The present work is devoted to the study of the sensitivity of the νCD stretching mode to conformations in the 2'-deoxyuridine deuterated on the (2'-R) position of the sugar ring (Compound **2**, Fig. 1).

Experimental

Preparation of the deuterated uridine and its derivative

Two methods were reported for the synthesis of 2′-deoxy-2′-deuterio-β-D-ribonucleosides. The first one involves Bu_3Sn^2H reduction of suitably 2′-functionalized ribonucleosides [17, 18]. The second involves a low yielding but stereochemically unambiguous multistep sequence starting from methyl 2,3-anhydro-β-D-lyxofuranoside [19]. To our knowledge none of these methods have been applied previously to uridine derivatives. We have chosen to perform radical chemistry methodology on the readily available 3′,5′-O-(1,1,3,3-tetraisopropyldisiloxan-1,3-diyl)-β-D-uridine, (TPDS-uridine) [20] after activation at O2′. The TPDS group was expected to reduce the conformational mobility of the sugar ring thus allowing both enhanced stereocontrol of the deuteration step and more easily reliable spectroscopic measurements. Reaction of phenoxychlorothionocarbonate under standard conditions [18] afforded the 2′-O-phenoxythiocarbonyl ester of TPDS-uridine which was further reduced with Bu_3Sn^2H in benzene solution (initiation by AIBN, at reflux temperature during one hour under argon). Although this sequence was claimed to afford up to 12% of the (2′-S)-[2′-^{2}H]-2′-deoxy epimer when it was applied to 3′,5′-O-TPDS-adenosine derivative [18], in our hands the transformation exhibited a far better selectivity. Although a small amount (*ca.* 10%) of non-deuterated derivative was detected, the (2′-R)-[2′-^{2}H]-2′-deoxy-3′,5′-O-TPDS-β-D-uridine, **1**, was the unique deuterated compound obtained. Further deprotection was conducted according to a standard method [20] to yield the free (2′-R)-[2′-^{2}H]-2′-deoxyuridine, **2**.

Spectroscopic techniques

Raman spectra. Two different multichannel spectrophotometers with an Ar^+ laser exciting source equipped with a microscope were used: a Dilor Microdil 28 and a Dilor XY. They enable the analysis of microcrystals of about 1.5 μm size. The solutions were studied with a Dilor Raman RTI 30 spectrophotometer equipped with an Ar^+ Spectra Physics laser and a triple monochromator. In this investigation, the 488 nm line of the Ar^+ laser was used.

The solution samples were of about 10–20 μl volume in cylindric tubes of 1 or 2 mm in diameter. The aqueous solutions of the nucleoside were saturated, i.e. at about 0.1 M concentration. For spectra in the 2200 cm^{-1} region, 15–40 scans were recorded.

IR absorption spectra. For absorption studies of films or solutions a FTIR Perkin Elmer 1720 spectrophotometer was used with ZnSe windows. The spectra were computed on a IBM PC-AT with the program "TRAV" (in ANL catalog, "Logiciels pour la chimie", Société Française de Chimie, Publ., 1990), elaborated in the Laboratoire de Spectrochimie Infrarouge et Raman.

NMR spectra. ^{1}H-NMR spectra of solutions were recorded at 250 MHz in the FT mode using a Bruker AM-250 spectrometer.

Results and Discussion

NMR results

(2′-R)-[2′-^{2}H]-2′-deoxy-3′,5′-O-TPDS-uridine (**1**). Our NMR ^{1}H analysis of this derivative in $CDCl_3$ solution gives for the vicinal protons the coupling constants $J_{1'-2'} = 1.0$ Hz and $J_{3'-4'} = 8.1$ Hz. To interpret these results, we have considered the studies reported on two different families of 3′,5′-cyclisized nucleosides.

The first one is that of cyclic-3′,5′-monophosphate-(2′-R)-[2′-^{2}H]-2′-deoxynucleosides in ^2H_2O solutions [17]. These conformationally constrained compounds show narrow ranges of coupling constants around $J_{1'-2'} \sim 1.5$ Hz and $J_{3'-4'} \sim 9$ Hz, which are compatible with an essentially constant conformation range of pseudorotational angle P in the limited sector 36°–54° of the N region and therefore are regarded as rigid single conformers [17, 21, 22].

The second family considered is that of a series of 3′,5′-O-TPDS-ribonucleoside derivatives [23]. These compounds in solution in organic solvents display a remarkably consistent range of coupling constants, $J_{1'-2'} = 1.4 \pm 0.2$ Hz and $J_{3'-4'} = 8.2 \pm 0.3$ Hz,

expressing a *trans* orientation of the H1′ and H2′ protons and therefore a β-type nucleoside with a strong preponderance of the N-type conformer, irrespective of the type of substituent at C1′ (base) and at C2′ [23]. This last independence property allows us to extend the above conclusions to the corresponding family of cyclic deoxyribonucleosides. Resulting from the 3′,5′ cyclisation, a relaxed C3′–C4′ region with a more flattened furanose ring, in the N-type conformation with a pseudorotation angle P in the 0–18° range, in equilibrium with a minor population of S-form, probably represents the best estimation of the conformation of these compounds in solution [23, 24]. The Altona–Sundaralingam numerical treatment [12] applied to the observed coupling parameters for the 3′,5′-O-TPDS-ribonucleoside derivatives gives a "best fit" for a 85% N-type (15% S-type) equilibrium composition, with pseudorotational parameter values, $P_N = 4.3°$, $\tau_{m,N} = 35.6°$ for the N-type conformer and $P_S = 170.4°$, $\tau_{m,S} = 36°$ for the S-type conformer [23].

The NMR results of compound **1** are entirely consistent with those displayed by the 3′,5′-O-TPDS-nucleosides family. Then, we conclude that compound **1** in chloroform is very nearly described as an equilibrium composition of 85% of N-form, with pseudorotational parameters close to the above reported values.

(2′-*R*)-[2′-^{2}*H*]-2′-*deoxy-β-D-uridine* (**2**). ^{1}H-NMR spectra of compound **2** in ^2H_2O solution give the coupling constants $J_{1'-2'} = 6.9$ Hz and $J_{3'-4'} = 4.0$ Hz. They are close to the values of GEORGE *et al.* [25] who found for deoxythymidine in ^2H_2O solution $J_{1'-2'} = 6.8$ Hz and $J_{3'-4'} = 4.1$ Hz. The coupling constants of **2** are consistent with a population of 63% of the S-type and 37% of the N-type conformers at equilibrium [12, 25–27], corresponding to the best fit calculated with the values of $P_S \sim 162°$, $\tau_{m,S} = 38°$ for the S-type conformer and $P_N \sim 9°$, $\tau_{m,N} = 38°$ for the N-type conformer, according to Altona and coworkers' treatments [12, 26]. Thus, our NMR measurements show that compound **2** in aqueous solution is in an N⇄S equilibrium substantially biased towards the S-type conformer (with a 63% population), in good agreement with all experimental investigations on deoxyribonucleosides [12].

Raman and FTIR vibrational spectra

Compound **1**. The Raman spectrum in the 2200 cm^{-1} region of **1** in solution appears either as a single band with a maximum at 2203 cm^{-1} in ethanol [Fig. 2(e)], 2197 cm^{-1} in butanol-1 and 2198 cm^{-1} in dimethylformamide, or as a doublet in chloroform, the same band at 2193 cm^{-1} being accompanied by a second weak band at 2238 cm^{-1} [Fig. 2(c)].

According to our NMR results giving a 85% population of the N conformer, the more important Raman band in chloroform solution, which is retrieved as a unique band in the other organic solutions, is assigned to the stretching mode νCD in the N conformer, while the minor band is assigned to the S conformer.

In the Raman spectrum of **1** in the crystalline state we find again the same feature as that observed in chloroform solution. The main band maximum at 2201 cm^{-1} and the shoulder at 2233 cm^{-1} are only slightly shifted ($\Delta\nu \leqslant 8$ cm^{-1}) from the solution maxima. They are assigned as in solutions.

In the FTIR absorption spectrum of a film of **1** [Fig. 2(g)], we recognize the νCD mode of the N conformer at 2195 cm^{-1}, among several overtones or combinations falling in the 2200 cm^{-1} range, which are probably due to the many supplementary modes expected for this much more complicated molecule compared to the non-cyclisized uridine.

Compound **2**. In the Raman spectrum of the aqueous solution two distinct νCD frequencies are observed at 2222 and 2201 cm^{-1}, the band of higher energy being the more intense one [Fig. 2(d)]. In ethanolic solution, these two bands are again observed at 2219 and 2192 cm^{-1} [Fig. 2(f)]. Compared to the Raman spectrum of **1** in the same solvent, ethanol [Fig. 2(e)], we can correlate the lower energy band of **2** at 2192 cm^{-1} to the single band of **1** at 2203 cm^{-1} and therefore to the νCD mode of the N conformer (see below, next section). The higher energy band at ~2220 cm^{-1}, corresponding to the weak

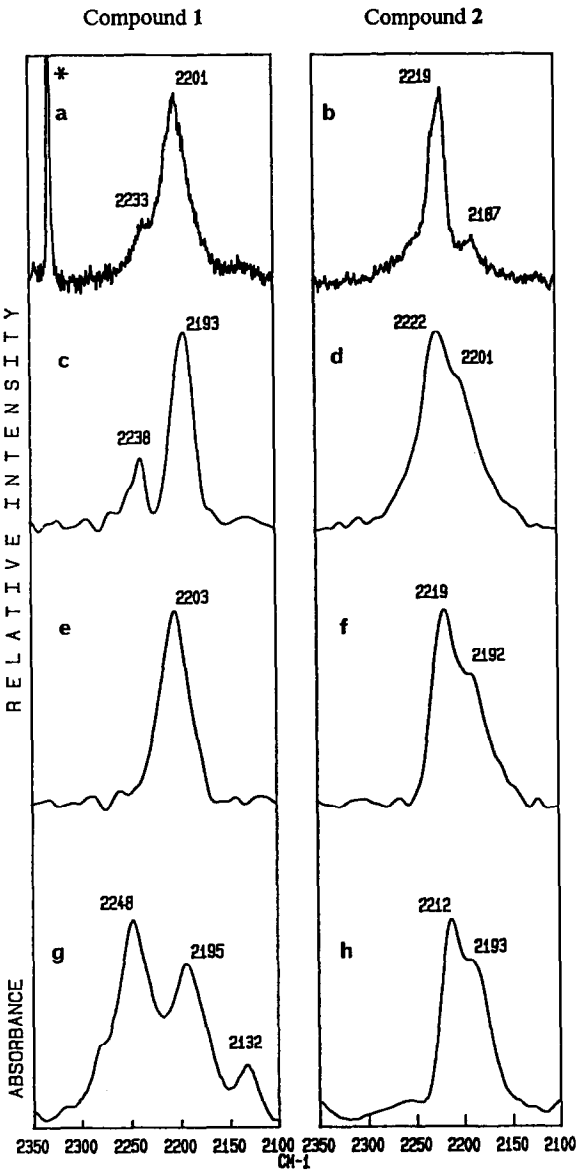

Fig. 2. Raman and FTIR spectra of compounds **1** and **2**. Compound **1**: Raman spectra: (a) solid state; (c) chloroform solution; (e) ethanol solution. FTIR spectrum of a film (g). Compound **2**: Raman spectra: (b) solid state; (d) aqueous solution; (f), ethanol solution. FTIR spectrum of a film (h). * A strong Raman line of N_2 of air appears at 2331 cm^{-1} due to the long integration time (1 h) applied for this spectrum.

band at 2238 cm^{-1} of **1** in chloroform solution, is then assigned to the νCD mode of the S conformer.

The Raman spectrum of **2** in the crystalline state exhibits a higher resolution of the bands and a different ratio of the intensities of the two bands compared to the solution. The two maxima appear at 2219 and 2187 cm^{-1}, instead of 2233 and 2201 cm^{-1} respectively for the cyclisized uridine [Fig. 2(b) and (a)]. The shift of the maxima of 14 cm^{-1} from **1** to **2**, as well as the 14 cm^{-1} shift observed for **2** from the aqueous solution to the crystalline state can be understood thanks to the analysis of the Raman bands by the technique of band decomposition (see next section). The important lowering of the relative intensity of the 2187 cm^{-1} N band in the crystalline state compared to the corresponding 2201 cm^{-1} N band in aqueous solution can be explained by an orientation effect of the crystal versus the polarization direction of the exciting laser line. It may also be due to a different conformer distribution in the crystal.

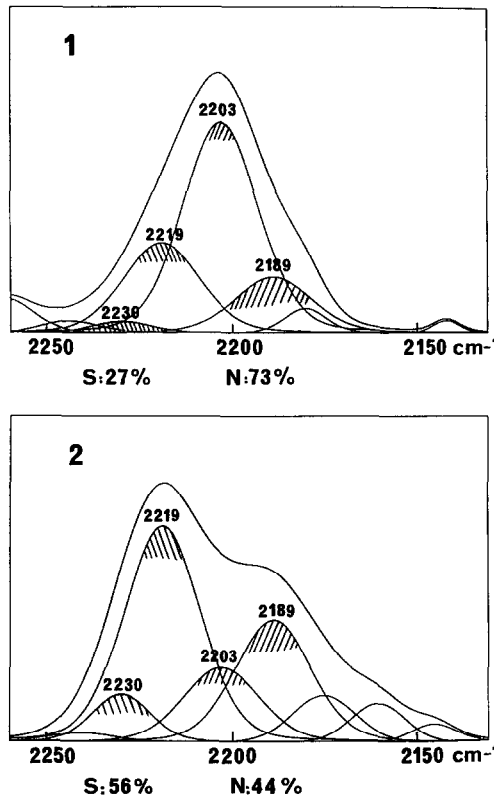

Fig. 3. Decomposition of the νCD Raman bands recorded in ethanolic solutions of compounds **1** and **2**. \\\: bands assigned to the C2'-endo conformer (S): in **1** 27%, in **2** 56%. ///: bands assigned to the C3'-endo conformer (N): in **1** 73%, in **2** 44%.

The FTIR absorption spectrum of a film of **2** shows two peaks at 2212 and 2193 cm^{-1} [Fig. 2(h)], only shifted by ~10 cm^{-1} from the Raman bands for the aqueous solution and by 7 cm^{-1} from the Raman bands for the crystal. This is compatible with an effect of the physical state.

Although the relative intensities of the Raman bands in the crystalline state cannot be directly related to the populations of the conformers, the crystalline state spectra have yet shown the coexistence of the two conformers and thanks to a higher resolution compared to the solution, have enabled us to assign unambiguously each of the two νCD modes to one of the two conformational forms of this nucleoside.

Decomposition of the νCD Raman bands of **1** *and* **2** *in solution*

By decomposition of the νCD Raman bands of **1** and **2** in ethanolic solution [Fig. 2(e) and (f)], we have found four components, common to both compounds, at the same wavenumbers, with equal widths and profiles (Fig. 3 and Table 1).

Apart from these four common bands, other bands arising from the decomposition are either weaker or do not occur at systematic wavenumbers for the two compounds and therefore are not assigned to the νCD modes of conformers but to high overtones or combinations of vibrational modes of lower frequency. Refining the assignments of the envelope bands described above, we are now able to correlate each of the N- and S-type conformers with a set of two components: the S-type conformer with the 2230 and 2219 cm^{-1} bands and the N-type conformer with the 2203 and 2189 cm^{-1} bands.

This complex structure of the band due to the νCD stretching mode for each conformer is in good agreement with the calculations of the potential energy of pseudorotation of the sugar ring [13, 28], giving a very flat area around the two potential minima; several close conformations may occur in each class of conformer, leading to "sub-states" revealed by modelling calculations [29] as well as experimental data [30].

Table 1. Assignments of the νCD Raman bands to the C2′-endo (S) and C3′-endo (N) conformers of the compounds **1** and **2** in different solvents; relative intensities of the Raman bands and populations of the conformers

		Raman band analysis						NMR results	
		Ethanol		Water		Chloroform		Water	Chloroform
Compound	Conformer	ν	Relative intensity %	ν	Relative intensity %	ν	Relative intensity %	Population %	Population %
1	S	2230	2 } 27			2238	15 } 18		15
		2219	25 }			2221	3 }		
	N	2203	58 } 73			2202	32 } 82		85
		2189	15 }			2189	50 }		
2	S	2230	8 } 56	2235	7 } 62			63	
		2219	48 }	2224	55 }				
	N	2203	17 } 44	2199	35 } 38			37	
		2189	27 }	2184	3 }				

The same technique of curve fitting has also been applied to the νCD Raman bands of **1** in $CHCl_3$ solution and **2** in aqueous solution [Fig. 2(c) and (d)].

Again we found the same two characteristic components for each type of conformer, only slightly shifted due to the solvent effect. The relative intensity of each band, together with the global relative intensity of each set of two bands assigned to a class of conformer, are reported in Table 1. We find distributions of Raman intensities over the two sets of bands very close to the populations calculated from our NMR coupling constants measurements: for **1** in chloroform solution, the Raman bands assigned to the S-form represent 18% of the overall νCD intensities, compared to a 15% population in the S-form deduced from our NMR measurements; for **2** in aqueous solution, the Raman bands assigned to the S-form represents 62% of the overall νCD intensity, compared to a 63% population in the S-form deduced from NMR. These close agreements allow us to conclude that the polarizabilities of the νCD modes of the S- and N-type conformers should be very close in magnitude.

The curve fittings of **1** also help us to understand the peculiar feature of the Raman spectrum in chloroform solution [Fig. 2(c)] compared to the other organic solutions spectra [Fig. 2(e)]: the enhancement of the two extremes of the four bands (at 2238 and 2189 cm^{-1}) in chloroform solution results in two well separated bands whereas in the other solvents the most intense bands being the two middle ones (at 2219 and 2203 cm^{-1}) (Table 1), they give rise to a one-band-like feature [Fig. 2(e)].

These observations show that within each class of conformers the proportion of the sub-states is reversed for **1** in chloroform solution compared to the other organic solutions and that the N⇄S equilibrium is displaced in favour of the N-class in chloroform compared to the other solvents with a 82% population instead of 73%.

These results may be compared to the IR and Raman study of cyclopentene-2-d_1 [31] in which the authors assign the two observed frequencies at 2167 and 2150 cm^{-1} to the νCD modes of the two conformers, the higher value corresponding to the more stable conformer.

The internal consistency of the relative intensities of the Raman bands through the compounds **1** and **2**, as well as the good general agreement of the Raman intensities with the conformer distributions measured by NMR for these two compounds support the validity of our assignments.

Conclusion

The uridine and its 3′,5′-O-TPDS-derivative have been specifically deuterated at the (2′-R) position for the first time. From the conformational distributions established by

proton NMR spectroscopy for these two compounds, we have been able to unambiguously assign each observed νCD frequency of the (2′-R)-deuterated-2′-deoxyuridine to one of the two classes of conformers, C2′-endo (S) and C3′-endo (N).

The band decomposition analysis led us to refine our assignments of these marker bands and to distinguish the existence of sub-states within each class of conformer.

These results encourage us in the belief that such selectively marked nucleosides, incorporated at specific sites of oligonucleotides could be good reporters of the local structure of double helices of DNA, free or complexed with proteins or drug molecules.

Acknowledgement—This work was supported in part by contract No. SCI-CT91-0705 (TSTS) from the European Economic Community to C.R.

REFERENCES

[1] H. P. M. De Leeuw, A. G. Haasnoot and C. Altona, *Isr. J. Chem.* **20**, 108 (1980).
[2] C. Altona, *Recueil, J. Royal Netherlands Chem. Soc.* **101**, 413 (1982).
[3] C. Altona, *Methods in Structural Molecular Biology* (Edited by D. B. Davies, W. Saenger and S. S. Danyluk), pp. 161–213. Plenum Press, London (1981).
[4] A. Bax and L. Lerner, *J. Magn. Reson.* **79**, 429 (1988).
[5] G. J. Thomas, Jr and A. H. J. Wang, *Nucleic Acids and Molecular Biology* (Edited by F. Eckstein and D. M. J. Lilley), Vol. 2. Springer-Verlag, Berlin (1988). G. J. Thomas, Jr, *Spectroscopy of Inorganic Bioactivators. Theory and Applications. Chemistry, Physics, Biology and Medicine* (Edited by T. Theophanides), pp. 247–263. Kluwer Academic (1989). Y. Nishimura, M. Tsuboi, T. Sato and K. Aoki, *J. Mol. Struct.* **146**, 123 (1986).
[6] R. E. Dickerson and H. R. Drew, *J. Mol. Biol.* **149**, 761 (1981).
[7] H. R. Drew, R. M. Wing, T. Takano, C. Broka, S. Tanaka, K. Itakura and R. E. Dickerson, *Proc. Natn. Acad. Sci. (USA)* **78**, 2179 (1981).
[8] R. Langridge, H. R. Wilson, C. W. Hooper, M. H. F. Wilkins and L. D. Hamilton, *J. Mol. Biol.* **2**, 19 (1960).
[9] R. Chandrasedaran, S. Arnott, A. Banerjee, S. Campbell-Smith, A. G. Leslie and L. Puigjaner, *ACS Symp. Ser. No. 141* 483 (1980).
[10] W. Saenger, *Principles of Nucleic Acid Structure*. Springer-Verlag, New York (1984); (a) p. 229, (b) p. 284, (c) p. 268, (d) p. 97.
[11] C. Altona and M. Sundaralingam, *J. Am. Chem. Soc.* **94**, 8205 (1972).
[12] C. Altona and M. Sundaralingam, *J. Am. Chem. Soc.* **95**, 2333 (1973).
[13] M. Levitt and A. Warshel, *J. Am. Chem. Soc.* **100**, 2607 (1978).
[14] S. Arnott and D. W. L. Hukins, *Nature* **224**, 886 (1969).
[15] H. Zine, A. Piart-Goypiron and M. H. Baron, *J. Mol. Struct.* **273**, 249 (1992).
[16] A. Piart-Goypiron, M. H. Baron, H. Zine, J. Belloc and M. J. Coulange, *Spectrochim. Acta* **49A**, 103 (1993).
[17] M. J. Robins, M. Mac Cross and J. S. Wilson, *J. Am. Chem. Soc.* **99**, 4660 (1977).
[18] M. J. Robins, J. S. Wilson and F. Hansske, *J. Am. Chem. Soc.* **105**, 4059 (1983).
[19] T. Pathak, H. Bazin and J. Chattopadhyaya, *Tetrahedron* **42**, 5427 (1986).
[20] W. T. Markiewickz, *J. Chem. Res. (S)* **24** (1979); *J. Chem. Res. (M)* 0178 (1979).
[21] M. Mac Cross, F. S. Ezra, M. J. Robins and S. S. Danyluk, *J. Am. Chem. Soc.* **99**, 7495 (1977).
[22] C. A. G. Haasnoot, F. A. A. M. de Leeuw, H. P. M. de Leeuw and C. Altona, *Org. Magn. Reson.* **15**, 43 (1981).
[23] M. J. Robins, J. S. Wilson, L. Sawyer and M. N. G. James, *Can. J. Chem.* **61**, 1911 (1983).
[24] C. H. Lee and R. H. Sarma, *J. Am. Chem. Soc.* **98**, 3541 (1976).
[25] A. L. George, F. E. Hruska, K. K. Ogilvie and A. Holy, *Can. J. Chem.* **56**, 1170 (1978).
[26] F. A. A. M. De Leeuw and C. Altona, *J. Chem. Soc. Perkin II* 375 (1982).
[27] D. B. Davies and S. S. Danyluk, *Biochemistry* **14**, 543 (1975).
[28] W. K. Olson and J. L. Sussman, *J. Am. Chem. Soc.* **104**, 270 (1982). W. K. Olson, *J. Am. Chem. Soc.* **104**, 278 (1982).
[29] M. Poncin, B. Hartmann and R. Lavery, *J. Mol. Biol.* **226**, 775 (1992).
[30] E. Taillandier, J. Liquier and M. Ghomi, *J. Mol. Struct.* **214**, 185 (1989).
[31] C. Rafilipomanana, D. Cavagnat, R. Cavagnat, J. C. Lassegues and C. Biron, *J. Mol. Struct.* **127**, 283 (1985). C. Rafilipomanana, D. Cavagnat and J. C. Lassegues, *J. Mol. Struct.* **129**, 215 (1985).